Open access • Journal Article • DOI:10.1029/96JB02654

Seismic triggering by rectified diffusion in geothermal systems — Source link

Bradford Sturtevant, Hiroo Kanamori, Emily E. Brodsky

Published on: 10 Nov 1996 - Journal of Geophysical Research (American Geophysical Union)

Topics: Induced seismicity, Pore water pressure and Earthquake swarm

Title

Seismic triggering by rectified diffusion in geothermal systems

Journal

Journal of Geophysical Research, 101(B11)

Authors

Sturtevant, Bradford
Kanamori, Hiroo
Brodsky, Emily E.

Publication Date

1996-11-10

Peer reviewed

JOURNAL OF GEOPHYSICAL RESEARCH, VOL. 101, NO. B11, PAGES 25,269-25,282, NOVEMBER 10, 1996

Seismic triggering by rectified diffusion in geothermal systems

Bradford Sturtevant

Graduate Aeronautical Laboratories, California Institute of Technology, Pasadena

Hiroo Kanamori and Emily E. Brodsky

Seismological Laboratory, California Institute of Technology, Pasadena

Abstract. Widespread seismicity was triggered by the June 28, 1992, Landers California, earthquake at a rate which was maximum immediately after passage of the exciting seismic waves. Rectified diffusion of vapor from hydrothermal liquids and magma into bubbles oscillating in an earthquake can increase the local pore pressure to seismically significant levels within the duration of the earthquake. In a hydrothermal system modeled as a two-component H_2O-CO_2 fluid in porous rock the pressure initially increases linearly with time. The rate of pressure buildup depends sensitively on the mean bubble radius and is large for small bubbles. The diffusion-induced pressure is relaxed by percolation and resorption of vapor into the liquid solution. The induced seismicity itself also relieves stress. Values of parameters used in the present calculations give results consistent with observations of triggered seismicity at Long Valley caldera after the Landers earthquake. For one representative condition, at 250°C and 5.6 km depth, oscillating strain acting on 10-μm-diameter bubbles increases pore pressure at the rate of 151 Pa/s resulting in a pressure increase of 12 kPa in the 80-s duration of the Landers earthquake. The elevated pressure induced by a single 26-m-diameter cloud of bubbles in saturated rock relaxes by percolation through soil of 0.2-mdarcy permeability in 53.6 hours. Observations of earthquake swarms at other locations suggest that self-induced buildup of pore pressure by rectified diffusion can provide a positive feedback mechanism for amplifying seismicity.

Introduction

Within minutes of the June 28, 1992, Landers California earthquake, seismicity abruptly increased across the western United States at sites as far as 1250 km (17 source lengths) from the epicenter [*Hill et al.*, 1993]. The triggered seismicity occurred primarily in regions of geothermal activity and recent volcanism. It is well known that human-induced alteration of geostatic stress by mining, well drilling, groundwater recharging, reservoir emptying or filling, and nuclear explosion induces local seismicity. In addition, cases of naturally triggered seismicity have previously been recorded. S. K. Singh et al., (Triggered seismicity in the valley of Mexico from major Mexican earthquakes, submitted to *Bulletin of the Seismolological Society of America*, 1996) have recently reported triggered seismicity in the record of the Valley of Mexico from coastal earthquakes at least 250 km away. They demonstrate that after the 1928 $M_w = 7.5$ Oaxaca earthquake, the two 1932 $M_w = 7.9$ and $M_w = 8.0$ Jalisco earthquakes, and the 1957 $M_w = 7.9$ Acapulco earthquake, seismicity increased significantly above background in the hydrothermally active Valley of Mexico. At Rabaul in Papua New Guinea there has been increased seismic activity after large earthquakes over 200 km away in the Solomon Islands [*Newhall and Dzurisin*, 1988]. An increase in seismic activity during August 1971 is linked to two $M_L = 8.0$ earthquakes in the Solomon Sea in July 1971. A March 1983 $M_S = 7.6$ earthquake at 200 km may be the cause of increased activity in August 1983. Most recently, a $M_S = 7.8$ quake on August 16, 1995, with an epicenter 260 km to the SE provoked a swarm of activity from August 16 through at least August 23. *Gomberg and Davis* [1996] document at least six separate events triggering seismicity at The Geysers, California from more than 200 km away.

The cause of naturally triggered earthquakes is not known; proposed mechanisms include tidal strain [*Klein*, 1976; *Rydelek et al.*, 1988] (see *Heaton* [1982] for contrary evidence), dike intrusion [*Hill et al.*, 1995], stress relaxation [*Rice and Gu*, 1983], aseismic slip [*Anderson*

Paper number 96JB02654.
0148-0227/96/96JB-02654$09.00

et al., 1994; *Bodin and Gomberg*, 1994], hydraulic pressure surge [*Johnston et al.*, 1995], increase of pressure due to buoyant rise of dislodged bubbles in magma [*Steinberg et al.*, 1989, *Linde et al.*, 1994], and liquefaction of magma [*Hill et al.*, 1993]. Processes which trigger seismicity may also trigger volcanic eruptions. Well-understood mechanisms of naturally excited pressure increase have the potential of contributing to understanding of the processes by which earthquakes initiate and the prediction of volcanic eruptions.

Hill et al. [1995] fit the cumulative seismicity observed at Long Valley caldera, California, less the background (5.8 events/d), to an exponential function, shown in Figure 1,

$$n_{\text{cum}} = 213\left(1 - e^{-0.54t}\right), \quad (1)$$

where t is time measured in days. The slope of this curve is the rate of the triggered seismicity, also shown in Figure 1. The rate is maximum immediately after passage of the Landers seismic waves, and decreases with a characteristic e-folding time of 1.85 days. This observation implies that the mechanism facilitating triggered seismicity is fully active immediately after passage of the Landers waves. In this paper we describe a process known as rectified diffusion, by which dynamic strain can rapidly increase pore pressure in a hydrothermal field. The objective is to determine the range of seismic and hydrologic parameters for which rectified diffusion increases pore pressure sufficiently rapidly to explain the onset of triggered seismicity at maximum rate within 1 min. of the arrival of the Landers main shock [*Michael*, 1992]. We consider mechanisms for the relaxation of pressure during and after seismic excitation, and we conclude by discussing the general implications of the concepts described in this paper. In a future paper we will report the range of conditions in magmatic systems which could lead to seismically significant increase of pressure in a body of magma and the potential for triggering volcanic activity.

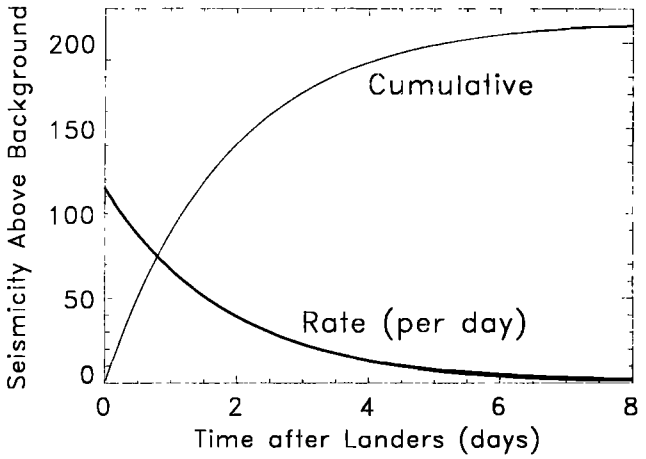

Figure 1. Cumulative seismicity at Long Valley caldera above the background level after the Landers earthquake.

Conceptual Model

In geothermal systems, fluid flow through thermal, compositional, and hydrostatic pressure gradients induces the separation of vapor (i.e., the formation of bubbles) and the precipitation of solids (deposition of minerals). Phase separation occurs, for example, when a gas dissolved in water becomes supersaturated. For simplicity, in this paper we consider the binary H_2O-CO_2 system. Vapor-liquid unmixing is moderated by surface tension; bubbles of radius r_c are stable only if the dissolved-gas concentration C_∞ is sufficiently large that the pressure of the vapor in the bubble withstands the tendency of surface tension to collapse the bubble. Once bubbles have formed, according to Henry's law the critical condition is given by [*Crum*, 1984]

$$\frac{C_\infty}{C_{\text{sat}}} = 1 + \frac{2\sigma}{r_c p_0}, \quad (2)$$

where C_{sat} is the saturation concentration, σ is the surface tension, and p_0 is the ambient pressure. The surface-tension-induced excess pressure inside the bubble, the "Laplace pressure," is $2\sigma/r_c$. At seismogenic depths, for example $p_0 = 150$ MPa, very small supersaturations are sufficient to permit the formation of stable bubbles. For example, with $\sigma = 0.07$ N/m, 10-μm-diameter bubbles are possible with only 0.01% supersaturation, and 0.1-μm-diameter bubbles are stable in the presence of 1% supersaturation. In this paper we assume that small regions containing CO_2-supersaturated water and bubbles occur randomly throughout geothermal systems.

The modeled geothermal system consists of fractured porous rock saturated with H_2O-CO_2 mixture (Figure 2). The medium is likely very heterogeneous, with seismic velocity, rock permeability and porosity, and pore pressure varying by large amounts over relatively small distances [*Johnston et al.*, 1995]. The dynamic strain imposed by seismic waves on the bubbly regions induces both sliding and dilatation of the fractures, fluid motion in the cracks, and deformation of the bubbles.

Oscillation of preexisting bubbles can rapidly increase the pore pressure of the system by rectified diffusion. During the expansion phase of the volume-changing component of oscillations (Figure 3a) the density of the gas-like phase in the bubbles is reduced, so it becomes undersaturated relative to the liquid-like phase, and dissolved gas diffuses into the bubble. During the compression phase the bubbles become supersaturated, and gas rediffuses back into the liquid (Figure 3c). For small, sinusoidal oscillations the saturation initially varies symmetrically about the initial value. However, the bubble surface area is larger during the expanded phase (Figure 3a) than during the compressed phase, so the total mass diffused into the bubble in one strain cycle is greater than the mass diffused out of the bubble. The vapor density in the bubbles steadily rises on a timescale long compared to the period of the seismic oscillation

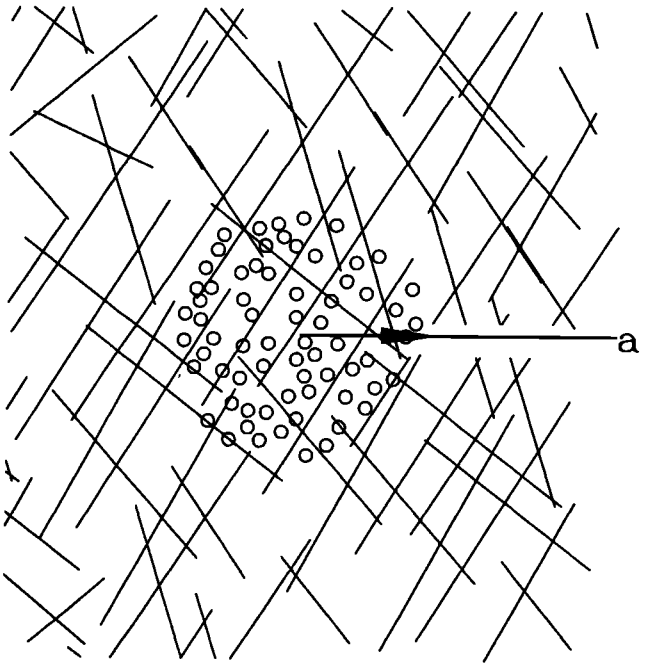

Figure 2. Schematic drawing of the model porous system with an idealized spherical accumulation of bubbles due to localized supersaturation.

[*Hsieh and Plesset*, 1961]. The net mass flux into the bubble is second order in the amplitude of oscillation, so the diffusion rate is proportional to the square of the amplitude of the dynamic seismic strain. The mass transfer takes place at constant temperature, and to the extent that the volume is constant, the increase of the density of the gas-like phase results in an increase of pressure in the neighborhood of the bubble. Thus rectified diffusion in an oscillating strain field tends to increase the pore pressure in bubble-containing regions.

Increased pore pressure reduces the effective normal stress, rendering existing faults more susceptible to Coulomb failure. In regions where the pore pressure is already moderately close to the normal stress the increase of pore pressure will cause the rock in or immediately adjacent to the bubbly region to fail, and triggered seismicity may occur. On the basis of observations of earthquake swarms induced by tidal strain we take the threshold value of pore pressure increase to trigger earthquakes to be 10 kPa (see below). The pressure generated by rectified diffusion induces failure only in the immediate neighborhood of the bubbly region. It probably does not directly contribute to deformation measured at the Earth's surface.

Volume-changing processes which allow the bubbles to grow and moderate the increase of pore pressure include elastic deformation and compaction of the surrounding rock and leakage of fluid out of the bubbly region through permeable rock. We show that percolation may serve to relax the pore pressure over timescales much longer than the duration of the remote earthquake. The triggered seismicity itself relaxes and redistributes the preearthquake stress state and the pore pressure elevated by rectified diffusion. If it is assumed that triggered seismicity occurs randomly with constant probability throughout the geothermal field, the number of pressurized regions triggering seismicity can be constrained.

Geothermal System

In the present model the geothermal field is composed of liquid-saturated fractured rock. Rectified diffusion is assumed to be active in roughly spherical regions that are small compared to the size of the field and sparsely distributed throughout it. The bubbles occur in small fractures and pores (Figure 2). We consider the excitation of this system by seismic surface and S waves. The shear wave velocity is dramatically reduced in the bubbly regions owing to both the presence of liquid and the large compressibility of the vapor phase.

While the wave propagation is modeled by a continuous medium with reduced shear velocity, the rectified diffusion process is treated by accounting for the small-scale motion of the liquid/vapor mixture in the rock matrix during seismic excitation. The macroscopic dynamic shear imposed on the system is accommodated at a small scale by (1) back-and-forth flow of liquid in the fractures and through the pores, (2) relative motion between the liquid and vapor phases, and (3) deformation of the bubbles by the rock motion and fluid flow. The enhanced macroscopic compressibility of regions in the geothermal system where phase separation has occurred is due almost entirely to deformation of the bubbles at microscopic scale; the rock and liquid are incompressible by comparison to the vapor. We do not treat the complex small-scale fluid motion induced by seismic waves in detail, but we assume that it leads to both shape and volume changes of the bubbles during shaking. That is, even though the macroscopic dynamic strain is principally by shear, at the microscopic scale,

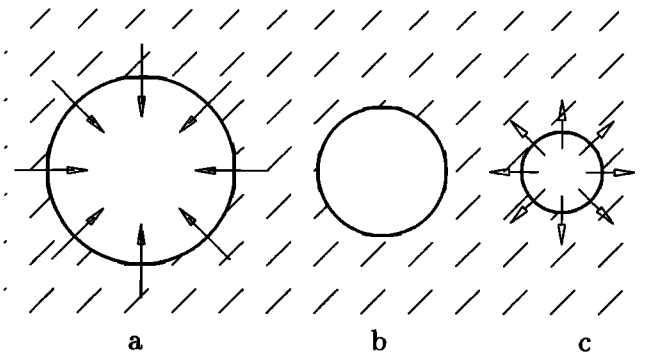

Figure 3. The mechanism of rectified diffusion. Oscillating bubbles in liquid (cross-hatched): (a) expanded phase, when the bubble is large and dissolved gas diffuses into the bubble, (b) equilibrium phase, when the vapor in the bubble is at saturated equilibrium with the dissolved gas, and (c) compressed phase, when the diffusive flow is out of the bubble.

bubble motions inevitably include dilatational oscillation, so rectified diffusion is induced. That dilatation is induced in aquifers by pure shear waves is proven by observations of deep wells, discussed below.

In a constant-volume, constant-temperature system an increase of vapor density in bubbles causes a proportionate increase of pore pressure in the immediate surroundings. Leakage of pressurized fluid through permeable rock in and around the bubbly region increases the volume of the system and relaxes the pore pressure. The permeability of the rock determines the time constant for relaxation of the pressure. Also, the pressure relaxes by rediffusion of the vapor that has been pumped into the bubbles back into the hydrothermal liquid. For rectified diffusion to be effective in triggering seismicity the times for fluid leakage and rediffusion must be larger than either the period of the seismic oscillation or the timescale for pressure buildup. Thus, as is the case for other theories of earthquake generation [*Gomberg and Davis*, 1996], it is necessary to have two disparate timescales, a short one for the facilitating process and a long one for the inhibiting process.

In the H_2O-CO_2 system, two immiscible fluid phases of contrasting density may coexist over a much larger range of pressure, temperature, and composition than is the case for pure H_2O. The critical point is raised from 22.1 MPa at 374°C to a maximum of more than 400 MPa (possibly as high as 5 GPa) at $T \approx 300$°C and $X_{CO_2} \approx 0.2$ [*Takenouchi and Kennedy*, 1964], where X is the mole fraction. Thus bubbles can exist at midcrustal depths. Real geothermal fluids are more complex than the simple binary mixture treated in this paper. Addition of NaCl to form the ternary mixture H_2O-CO_2-NaCl, a realistic model of geothermal fluids at depth, further increases the domain in (p, T, X) space in which immiscible phases coexist. A high-pressure, high-temperature region in which an NaCl-rich liquid (brine) coexists with an H_2O-CO_2-rich fluid connects with the region of mixed H_2O-rich liquid and CO_2-rich vapor at lower p and T, substantially increasing the upper limit of the immiscibility gap [*Bowers and Helgeson*, 1983]. A well-known consequence of this fact is that immiscible phases are commonly found in geothermal and magmatic systems.

The binary H_2O-CO_2 system treated here is sufficient to yield an order-of-magnitude estimate of the quantitative effects of rectified diffusion for temperatures to 250°C. For higher temperatures (to 500°C or more) it is necessary to model the system as a ternary system. However, in view of the fact that borehole measurements at Long Valley [*Sorey and Farrar*, 1992] indicate that the temperature does not exceed 250°C and remains rather constant with depth, we consider only the binary model in this paper.

Analytical Model

We consider an assemblage of N bubbles localized in an idealized spherical subregion of radius a (Figure 2). In this section we take the bubbles to all have the same radius r. The total volume V of vapor in the bubbly region is

$$V = NV_b , \tag{3}$$

where $V_b = \frac{4}{3}\pi r^3$ is the volume of a single bubble. In Appendix A we show how the theory can be modified to treat an arbitrary distribution of bubble sizes and how rectified diffusion causes small bubbles to grow at the expense of large bubbles.

Rectified Diffusion

Hsieh and Plesset [1961] developed a theory of rectified diffusion for spherical bubbles oscillating with small amplitude. The theory assumes (1) that the frequency of the imposed oscillatory stress field is large compared to the rate of increase of mass in the bubbles, so the effect of the oscillations can be averaged over many cycles to yield an effectively constant rate of diffusion and (2) that the fluctuating diffusion-depleted layer in the liquid adjacent to the bubble is much thinner than the bubble diameter. For the purpose of calculating the difference between the dissolved concentration in the depleted layer and in the undisturbed liquid, Hsieh and Plesset assume that Henry's law holds; that is, at constant temperature the concentration of dissolved gas in the liquid at the liquid-vapor interface is proportional to the pressure in the bubble. Hsieh and Plesset solve the forced diffusion equation with appropriate boundary conditions for the average mass flux $\dot{m}$ into a bubble of radius r_0 by a method of successive approximation, with the result

$$\dot{m} = 24\pi DC_\infty r_0 \delta^2 , \tag{4}$$

where overdot designates the time derivative, D is the diffusion coefficient, C_∞ is the saturated mass concentration (mass/volume) of the volatile in the undisturbed liquid, and δ is the dynamic seismically induced fractional change of bubble radius. Equation (4) (or dimensional reasoning) shows that the rate of increase of vapor density, given by the mass flux divided by the bubble volume, is inversely proportional to the square of the bubble diameter. Small bubbles induce larger rates of change of pressure than do large bubbles because their density increases more rapidly. Therefore it is likely that rectified diffusion first generates seismically significant pressure during an earthquake in localized regions where the scale of unmixed phases is small, presumably because phase separation has been affected by geothermal or geochemical processes.

The number of moles of vapor in the bubble increases at the rate

$$\dot{n} = \frac{\dot{m}}{M_v} , \tag{5}$$

where M_v is the molar mass of the vapor. Normalizing with the number of moles n_0 initially in the bubble, given by the equation of state of a perfect gas averaged over many oscillations of the bubble,

$$p V_b = nRT , \tag{6}$$

where R is the gas constant, we get

$$\frac{\dot{n}}{n_0} = \frac{\dot{m}}{V_{b0}} \frac{RT_0}{M_v p_0} . \tag{7}$$

The initial state in the geothermal system before arrival of the seismic waves is denoted by subscript zero. With (4), the rate of increase of the density in the bubble by rectified diffusion becomes

$$\frac{\dot{n}}{n_0} = \frac{K}{r_0^2} , \tag{8}$$

where

$$K = \frac{RT_0}{M_v p_0} 18 DC_\infty \delta^2 . \tag{9}$$

For simplicity, the vapor phase has been assumed to be a perfect gas, though at elevated p and T it could equally well be represented more accurately by using, for example, the modified Redlich-Kwong equation of state [*Flowers*, 1979]. The heat content of the liquid and solid phases is much larger than that of the vapor, so exsolution takes place at nearly constant temperature.

Percolation

The model system treated here is a permeable, fluid-saturated basin (Figure 2), within which pressure increase in bubbly regions causes the interstitial fluid to percolate outward into the field, resulting in a moderation of the pressure rise. Because the vapor phase in the bubbly regions is much more compressible than liquid or rock, we ignore elasticity [*Rice and Cleary*, 1976; *Delaney*, 1982] and compaction of the containing rock [*Scott and Stevenson*, 1986] and compressibility of the liquid. In Appendix B we show how liquid compressibility can be accounted for in the theory.

It is assumed that departures from the initial state, are small. Then, differentiating (6), the vapor equation of state, with respect to time yields

$$\frac{\dot{p}}{p_0} = -\frac{\dot{V}_b}{V_{b0}} + \frac{\dot{n}}{n_0} . \tag{10}$$

The term in $\dot{n}$ has been derived above for rectified diffusion, and that result applies independently of the magnitude of the $\dot{V}_b$ term, so long as the changes remain small. The rate of change of bubble volume $\dot{V}_b$ is due to leakage of fluid out of the pressurized region. We assume that the bubbles are distributed uniformly throughout the bubbly region and henceforth treat the three-phase rock/liquid/vapor region as a continuum. Neglecting any creation or destruction of bubbles during the earthquake (N = const), multiplying the numerator and denominator of the first term on the right-hand side of (10) by N and using (3) and (8) gives

$$\frac{\dot{p}}{p_0} = -\frac{\dot{V}}{V_0} + \frac{K}{r_0^2} . \tag{11}$$

By continuity, the relative rate of change of volume of the vapor phase is equal to the divergence of the velocity u_r of hydrothermal fluid through the fractured rock matrix,

$$\frac{\dot{V}}{V} = \nabla \cdot u_r , \tag{12}$$

where by Darcy's law,

$$u_r = -\frac{\kappa}{\eta} \frac{\partial p}{\partial r} . \tag{13}$$

In the assumed spherically symmetric system (Figure 2) the percolation velocity u_r is radial. The parameter κ is the permeability of the porous medium, and η is the viscosity of the fluid. Substituting (12) and (13) into (11) gives a diffusion equation for p

$$\frac{1}{p_0} \frac{\partial p}{\partial t} - \frac{\kappa}{\eta} \frac{1}{r^2} \frac{\partial}{\partial r} \left(r^2 \frac{\partial p}{\partial r} \right) = \frac{\dot{p_0}}{p_0} , \tag{14}$$

where

$$\dot{p_0} = \text{const} \equiv \frac{K p_0}{r_0^2} = \frac{RT_0}{M_v} \frac{18 DC_\infty \delta^2}{r_0^2} . \tag{15}$$

Solution

The solution of Equation (14) is given by *Carlslaw and Jaeger* [1959, equations. 13.9(13) and 13.9(14)]. The pressure at the center of the bubble cloud $p(0,t)$ is the largest in the field [*Carlslaw and Jaeger*, 1959, equation 13.9(12)],

$$p(0,t) = p_0 + p_{\max} \left[1 + \left(\frac{1}{2y^2} - 1 \right) \operatorname{erf} y - \frac{1}{\sqrt{\pi} y} e^{-y^2} \right] , \tag{16}$$

where erf is the error function and

$$p_{\max} = \frac{a^2}{2\kappa/\eta} \frac{\dot{p_0}}{p_0} , \qquad y = \frac{a}{2\sqrt{p_0 (\kappa/\eta)\, t}} . \tag{17}$$

The variable y is the square root of the ratio of the characteristic time for percolation to t. Figure 4 is a plot of $(p(0,t) - p_0)/p_{\max}$ versus the nondimensional time $1/y^2 = 2p_0 \kappa t / \eta a^2$. For small time ($y \gg 1$),

$$p(0,t) - p_0 \doteq \frac{p_{\max}}{2y^2} = \dot{p_0}\, t ; \tag{18}$$

the pressure initially increases linearly at the rate $\dot{p_0}$ in response to the increase of bubble vapor density by rectified diffusion. For large times ($y \ll 1$) the pressure gradually approaches a constant value

$$p(0,t) - p_0 = p_{\max} = \frac{a^2}{2\kappa/\eta} \frac{\dot{p_0}}{p_0} ; \tag{19}$$

after a time of order

$$\tau = \frac{a^2}{4 p_0 \kappa/\eta} , \tag{20}$$

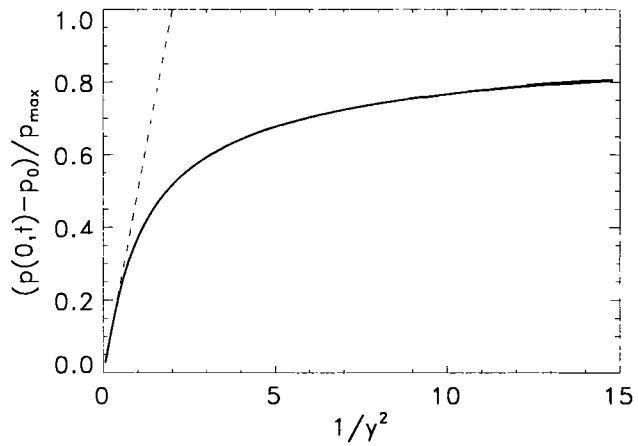

Figure 4. Normalized pressure at $r = 0$ versus normalized time. The small-time asymptote (equation (18)) is indicated by the dashed curve. The large-time asymptote, $(p - p_0)/p_{\max} = 1$, is approached only very slowly.

the characteristic time for percolation out of the bubbly region, the effect of leakage is felt at $r = 0$, and pressure eventually levels off to $p_{\max}$ for as long as the forcing oscillation persists. For the calculations carried out in this paper the percolation time is actually much larger than the duration of the earthquake, $\tau \gg \Delta t$ so the steady state is never approached, and the small-time result (18) holds.

The parameter p_{max} is the product of the rate of pressure increase by rectified diffusion $\dot{p}_0$ and the percolation time τ. The parameter $\dot{p}_0$ contains only variables pertaining to rectified diffusion and dynamic strain: D, C_∞, r_0, T_0, and δ. It depends strongly on the bubble size r_0 and the dynamic strain δ (see below). It is proportional to the concentration of dissolved vapor C_∞, the temperature T_0, and the diffusion coefficient D. It depends on the coexistence of unmixed phases but only indirectly on the details of how they are configured in the containing rock.

Pressure Relaxation by Percolation and Resorption

After the oscillatory seismic excitation ceases, percolation continues, so the induced pressure decreases. Considering only this process, the time it takes the pressure to return to ambient is τ, the characteristic time for percolation (equation (20)).

In addition, the vapor resorbs from the bubbles back into the liquid phase in a process limited by the diffusion coefficient D, the bubble diameter r_0, and the amount that the system has been driven out of equilibrium. This process was studied by *Epstein and Plesset* [1950], who derived an expression for the time it takes the vapor in a bubble to dissolve into the liquid,

$$t_r = \frac{r_0^2}{2} \frac{\rho_v}{D(C_{v\,\mathrm{sat}} - C_\infty)}, \qquad (21)$$

where $C_{v\,\mathrm{sat}}$ is the saturated concentration of vapor in the liquid corresponding to ρ_v, the elevated density of vapor in the bubble generated by rectified diffusion. Equation (21) is the large-time approximation to the solution of the diffusion problem, appropriate for the current calculations. Embodied in the approximation is the stipulation that the steady diffusion-depleted layer is thick compared to the bubble radius. The characteristic time $\tau_{\mathrm{layer}} = r_0^2/D$ for the diffusion-depleted layer to become equal to the bubble radius for a 10-μm-diameter bubble is $\sim$0.006 s. For the small changes generated by seismic excitation we assume that Henry's law holds; that is,

$$\frac{C_{v\,\mathrm{sat}}}{C_\infty} = \frac{\rho_v}{\rho_{0v}} = 1 + \frac{\dot{m}\,\Delta t}{\rho_{0v} V_0}, \qquad (22)$$

where ρ_{0v} is the initial vapor density in equilibrium with C_∞ and Δt is the duration of the seismic excitation. Using (22) and (4) in (21), and setting to first order $\rho_v \doteq \rho_{0v}$ in the numerator of (21) yields

$$t_r = \frac{1}{\Delta t}\left(\frac{r_0^2\,\rho_{0v}}{6\,D\,C_\infty\,\delta}\right)^2 = \frac{p_0^2}{\dot{p_0}^2}\frac{1}{\Delta t}. \qquad (23)$$

The resorption time t_r depends sensitively on all of the parameters controlling diffusion into and out of bubbles. For the conditions considered in the calculations described below, the resorption time is always much larger than the percolation time.

Seismological Considerations

The dynamic strain induced by the Landers earthquake at Long Valley, California, is estimated from a seismogram recorded with an accelerograph at the Mammoth Lakes Airport, Long Valley (MLAC: latitude, 37.634°; longitude, -118.838°; epicentral distance, $\Delta_{\mathrm{MLAC}} = 3.9°$; azimuth, 330°). Figure 5 shows the three-component ground-motion velocity record. Unfortunately, the record is cut off at about 30 s after the onset of the surface wave. However, the general behavior of the ground motion (duration and amplitude) after the record is cut off can be estimated using the record from a TERRAscope station at Lake Isabella (ISA: latitude, 35.643°, longitude, -118.480°; epicentral distance, $\Delta_{\mathrm{ISA}} = 2.2°$; azimuth, 311°) shown in Figure 6.

At ISA the duration of the large-amplitude motion is about 50 s, and the peak-to-peak ground-motion velocity is about 8 cm/s on the E-W component and 5 cm/s on the vertical component. Since the distance to MLAC is about twice that to ISA, the duration of signal at MLAC is expected to be considerably longer. If the minimum and the maximum group velocities are $U_{\min}$ and $U_{\max}$, respectively, the duration at MLAC should be longer than that at ISA by $(\Delta_{\mathrm{MLAC}} - \Delta_{\mathrm{ISA}})(1/U_{\min} - 1/U_{\max})$. If we assume $U_{\min} = 2$ km/s and $U_{\max} = 3$ km/s, reasonable values for crustal surface waves, the duration at MLAC is estimated to be about 80 s.

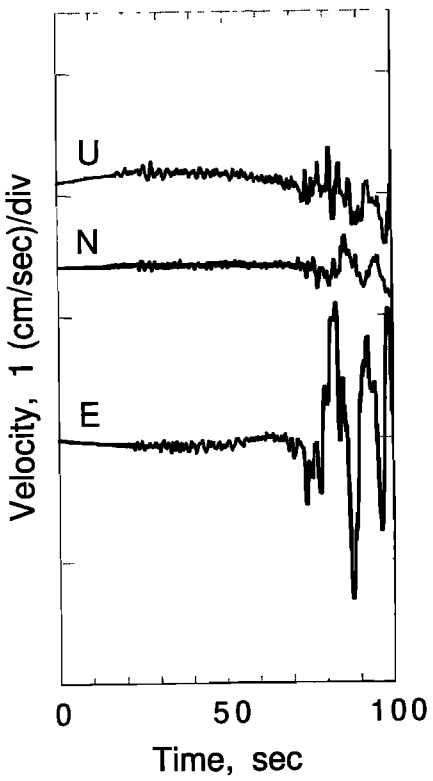

Figure 5. Three-component ground-motion velocity record from Mammoth Lakes Airport, Long Valley, California (MLAC): $\Delta = 3.9°$, $\phi = 331°$.

Since the Landers earthquake is strike slip with a strike of about 340°, the large-amplitude wave recorded on the E-W component at MLAC is a Love wave. The Rayleigh wave is expected to be relatively small at MLAC, but the record seems to be cut off before the arrival of the peak of Rayleigh wave train. Judging from the difference in azimuth between MLAC and ISA and the amplitude of the Rayleigh wave at ISA (vertical component), we estimate that the Rayleigh to Love wave amplitude ratio at MLAC is about 1/3. Then the dynamic strain ϵ can be estimated from the integrated acceleration by

$$\epsilon = \frac{\dot{u}}{c}, \tag{24}$$

where c is the phase velocity. Assuming $c = 2.2$ km/s, we obtain $\epsilon_{\mathrm{MLAC}} = 5.6 \times 10^{-6}$ and 1.9×10^{-6} from the horizontal and the vertical components, respectively. These are the shear and longitudinal linear strains, respectively. The value for the shear strain is comparable to that reported by *Hill et al.* [1993].

The strain was measured at the surface. However, since the wavelength of the observed surface waves with a period of 10 s is about 30 km and the skin depth (the depth of energy penetration) of surface waves is approximately 1/3 of the wavelength, we conclude that the strain estimated at the surface is representative of deformation at depths of from 0 to 10 km, where much of the triggered seismicity occurred.

As the wave enters a soft, low-velocity hydrothermal zone consisting of crushed rock, liquid, and vapor, by conservation of energy the strain is amplified by the square root of the ratio of acoustic impedances $Z = \rho V_s$,

$$\epsilon = \sqrt{\frac{Z_{\mathrm{MLAC}}}{Z}}\,\epsilon_{\mathrm{MLAC}}, \tag{25}$$

where V_s is the shear wave velocity. The effect on V_s of bubble-rich fluid-saturated rock at depth is not known. Though a large-scale regional tomographic image of S wave velocity in Long Valley [*Romero and McEvilly*, 1993] shows that the lowest value of V_s in the top 2 km is 1000 to 1500 m/s, it is likely that in localized vapor-containing regions the shear velocity will be very much lower. V_s is reduced relative to dry rock both owing to the presence of liquid and of a highly compressible phase, vapor in the bubbles. *Kieffer* [1977] showed that the longitudinal wave velocity in bubbly water can be as low as 1 m/s. We expect that the presence of bubbles in fluid-saturated rock will have a correspondingly large effect, and as a model of this situation at depth, we use available information about the shear wave velocity of shallow wet, porous soil. *Puzyrev and Kulikov* [1980] show that $V_s = 30$–50 m/s in water-saturated deposits. *Addo and Roberston* [1992] report values of V_s as low as 40–50 m/sec at shallow depths (to 10 m) in sand and soft clay. For lake bed sites at Mexico City, *Singh et al.* [1988] estimate that $V_s > 58$ m/s at depths to below 58 m. In the Imperial Valley, $V_s = 350$ m/s to a depth of 105 m [*Liu*, 1983]. For a soft, low-velocity hydrothermal zone consisting of crushed rock, liquid, and vapor we take $c = 200$ m/s and density $\rho = 70\%$ of that of the rock at MLAC. Using (25), the result is $\epsilon = 2.2 \times 10^{-5}$. This estimate of the effects of local conditions at depth in a hydrothermal field yields values about one half of the synthetic dynamic strain from the Landers earthquake computed by *Anderson et al.* [1994] at the hypocenter of the June 29, 1992, Little

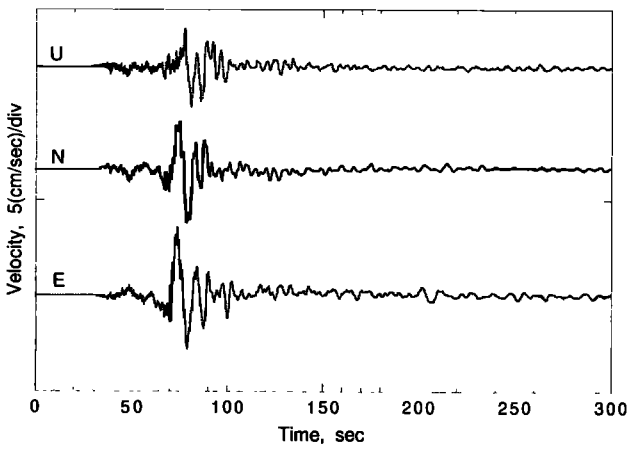

Figure 6. Three-component ground-motion velocity record from Lake Isabella, California (ISA): $\Delta = 2.2°$, $\phi = 311°$.

Skull Mountain earthquake, which was triggered by the Landers earthquake. It is 2 orders of magnitude smaller than strain observed in saturated lake bed sediments at Mexico City during the September 19, 1985, Michoacan earthquake [*Singh et al.*, 1988].

If the medium is extremely heterogeneous, a significant portion of the shear strain can contribute to volume change. For example, several investigators [*Sterling and Smets*, 1971; *Rexin et al.*, 1962; *Carragan et al.*, 1964] have demonstrated that the water level of some deep wells changes synchronously with teleseismic Love and S waves. The most convincing cases are presented by *Carragan et al.* [1964] in which direct comparisons are made between well records and inertial seismograph records. *Carragan et al.* [1964, p. 37] state that "Qualitatively, the Love waves have similar amplitudes relative to Rayleigh waves on well records and on inertial records; this suggests a strong volume effect associated with these waves, which is not yet understood." In one of the examples [*Carragan et al.*, 1964, Figure 19A] they compare Love waves from a Chinese earthquake ($\Delta = 106°$, $m_b = 6.1$) recorded with a water well seismograph at Saratoga Springs, New York, (15 cm diameter and about 100 m deep) and with an inertial seismograph at Troy, New York. From the record of the inertial seismograph we can estimate that the shear strain of a Love wave at a period of 80 s is approximately 5×10^{-10}. The same Love wave produced a water level change of approximately 0.005 cm, or a volume change of 0.9 cm^3 (relative volumetric change equal to 1.3×10^{-7}), suggesting significant shear to longitudinal strain conversion. The complex geometry of the aquifer system is probably responsible for this conversion. We note, however, that *Blanchard and Byerly* [1935] found no positively identifiable Love waves on water level records. Coseismic oscillations of at least 20-cm amplitude in wells at Long Valley caldera were observed during the Landers earthquake by *Roeloffs et al.* [1995]. Assuming an efficient conversion, the shear strain calculated above is taken to be the magnitude of the volumetric strain. For an order-of-magnitude estimate of the fractional change of bubble radius δ we take $\delta \sim \epsilon = 2.2 \times 10^{-5}$.

Finally, to measure the magnitude of the pressure increase caused by rectified diffusion, it is necessary to specify a threshold above which earthquakes can be triggered. That tidal strains are sufficient to trigger earthquakes in individual swarms or aftershock sequences has been shown in several studies. *Matuzawa* [1964] and *Mauk and Kienle* [1973] show that tidal strain can alternately turn seismicity on and off or strongly modulate the seismicity rate in a cluster. *Klein* [1976] and *Sauck* [1975] show that earthquakes as large as $M_L = 5.5$ were triggered in synchronism with Earth tides during the 1975 Brawley swarm. In this work, for the purpose of judging the effectiveness of rectified diffusion in triggering seismicity, we take the threshold of pore pressure increase to be 10 kPa, significantly larger than the normal stress corresponding to tidal strain, approximately 1 kPa.

Calculations

The rate of pressure rise $\dot{p}_0$ induced by rectified diffusion and the time for relaxation of the pressure τ have been calculated for the H_2O-CO_2 system for a range of ambient pressure (depth) and temperature and for representative values of the controlling parameters. We present plots of calculated values of $\dot{p}_0$ and τ for a range of thermodynamic conditions representative of Long Valley caldera. In order to give a quantitative sense of the consequences of rectified diffusion at each stage in the calculation we cite numerical results for one representative thermodynamic state, namely, $p = 150$ MPa and $T = 250°C$. However, it should be noted that rectified diffusion is effective in any unmixed liquid-vapor system, so it is actually effective over a very wide range of temperature and depth. Other input parameters to the calculations are $r_0 = 5$ μm and $\Delta t = 80$ s, which yield pore pressure increases sufficient to meet the 10-kPa failure criterion established above, and $a = 13$ m and $\kappa = 0.2 \times 10^{-15}$ $m^2 = 0.2$ mdarcy, which yield percolation times consistent with observations of the duration of triggered seismicity at Long Valley. *Sorey et al.* [1978] quote values of permeability obtained from wells from 50 to 300 m deep at Long Valley caldera in the range 7×10^{-19} to 8×10^{-12} m^2. The value we have used for κ is a factor of 10 smaller than the middle of the observed range, suggesting that those source regions which triggered late in the swarm may have been relatively well sealed in comparison with others. Since the permeability is not well constrained, we do not consider any relatively small changes that might be caused by the seismic shaking itself. The ambient pressure p_0 is taken to be lithostatic pressure under rock of density 2750 kg/m^3 (for example, 150 MPa at 5.6 km depth).

The variation of C_∞ with p and T in the saturated H_2O-CO_2 system is complex, so the calculations are made only at p and T for which experimental equilibrium concentration data are available. We use tabulated data of *Wiebe and Gaddy* [1940] and *Takenouchi and Kennedy* [1964]. For this reason the plotted results are not smooth; they reflect the scatter of the experimental data. However, when isotherms cross at low pressure the effect is real; the calculated quantity has the same value at two different temperatures. Data to 300 MPa (11 km) for the binary H_2O-CO_2 system are available in graphical form [*Takenouchi and Kennedy*, 1964]. However, for these depths the possibility that temperatures are higher than 250°C should be considered, so a ternary system such as H_2O-CO_2-NaCl must be treated. For the sake of simplicity and clarity of concept we limit the calculations to depths less than 5.6 km and use the simpler binary system. In view of the independence of depth at temperatures less than 250°C exhibited by the calculations, results from this simplified

model are representative of behavior at greater depth.

In order to calculate C_∞ from the measured values of mole fraction X the density of the liquid phase ρ_l is required. For the purpose of determining C_∞ we take ρ_l to be 1000 kg/m^3, though a more accurate approximation could be made by using the density of pure water given in thermodynamic tables; over the range of (p, T) used in these calculations the density of water can be as low as 650 kg/m^3 (at $p = 20$ MPa, 740 m depth, and $T = 350$°C). X measured by *Wiebe and Gaddy* [1940] at 50°C and 75°C is extrapolated to obtain the $T = 100$°C isotherm. Values at 250°C and 5.6 km depth (150 MPa) are $X = 0.54$ and $C_\infty = 291$ kg/m^3.

In order to calculate the percolation velocity the viscosity of the liquid phase must be known. In these calculations the viscosity of pure water $\eta_{H_2O}(p, T)$ [*Haar et al.*, 1984] is used as an estimate. For $T = 150$°–250°C, the data of *Haar et al.* [1984] are extrapolated from 100 MPa to 150 MPa. The value at 250°C and 5.6 km depth is $\eta = 1.4 \times 10^{-4}$ Pa s. The diffusion coefficient for CO_2 in the liquid phase is calculated from the viscosity of water using a modified Einstein relation verified experimentally over a temperature range of 0°–65°C by *Himmelblau* [1964, equation 89]. A typical value extrapolated to 250°C and a depth of 5.6 km is $D = 1.5 \times 10^{-8}$ m^2/s.

Results

Figures 7 and 8 show isotherms of $\dot{p}_0$ and τ resulting from seismic excitation of small (10 μm diameter) compressible inclusions in the H_2O-rich phase of a saturated mixture of H_2O-CO_2. Results for other values of the input parameters may be obtained by scaling the plotted results according to (15) and (20) and the equations upon which they depend. The isotherms of Figure 7 exhibit the typical bifurcation pattern of binary mixtures, in which high-temperature isotherms approach and cross the critical line (indicated by asterisks) into the CO_2-rich phase (not shown), while the low-temperature isotherms bend parallel to the critical line and remain separated by the immiscibility gap from their counterparts in the CO_2-rich phase [*Takenouchi and Kennedy*, 1964, Figure 8]. For a fixed value of dynamic strain the low-temperature isotherms are independent of depth in the range 100–200 MPa (3.7–7.4 km).

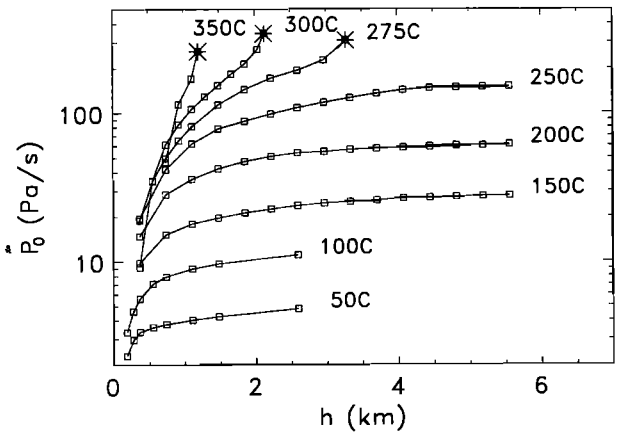

Figure 7. Isotherms of the initial rate of pressure rise as a function of depth. The endpoints of the curves marked with asterisks lie on the critical curve of the binary system.

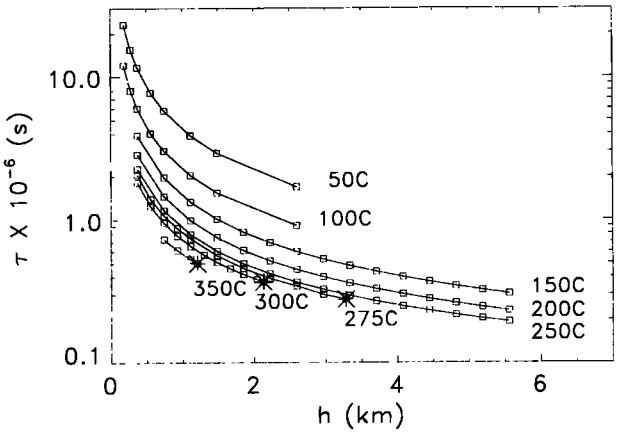

Figure 8. Isotherms of the time required for the effects of percolation to become significant (equation (20)) versus depth.

Figure 7 demonstrates that with the values of the parameters used in the calculation, rectified diffusion into small inclusions is sufficient to induce seismically significant changes of pore pressure (10 kPa) during the shaking. For example, at 250°C and 5.6 km depth oscillating volumetric strain of amplitude 2.2×10^{-5} acting on bubbles of 10 μm diameter increases pressure at the rate of 150.8 Pa/s, resulting in a pore pressure increase of 12.1 kPa in the 80-s duration of the earthquake. Figure 8 shows that for the values of the parameters used in these calculations, percolation does not limit the pressure achieved during shaking times of seismic interest and that the induced pressure relaxes at 250°C and 5.6 km in 1.93×10^5 s (53.6 hours). This value is consistent with the duration of triggered seismicity at Long Valley after the Landers earthquake [*Hill et al.*, 1995]. Under cooler conditions the holding time is longer.

The triggered seismicity itself relaxes and redistributes preexisting stress in the seismogenic region and pressure induced by rectified diffusion. The development in time of triggered seismicity (Figure 1) gives information about the relaxation process. The total number of triggered earthquakes counted by (1) is 213, and the rate decreases exponentially, as shown in Figure 1. By the rectified diffusion mechanism the seismic waves from a remote earthquake pressurize a number of small regions distributed throughout the hydrothermal system. Equation 1 can be interpreted in terms of the model as follows. We interpret the asymptotic limit in (1) to be the number of bubbly regions which have been pressurized sufficiently to eventually trigger an earthquake; that is, $N_r = 213$. Let P be the prob-

ability that rock in the neighborhood of a pressurized locality will fail in a given time interval Δt. That is, the expected time to failure is $1/P$. We assume that all of the triggered events result from the initial excitation. Then the expected number of triggered events during the first time interval Δt is $N_r P$. During the next time interval it is $N_r P(1-P)$, and in the mth time interval, between times $m\Delta t$ and $(m+1)\Delta t$ the expected number of events n_e is

$$n_e(t = m\Delta t) \;=\; N_r P(1-P)^m \;, \qquad (26)$$

a geometric distribution. Similarly, equation (1) implies that in an interval between times $m\Delta t$ and $(m+1)\Delta t$ the number of events n_e is approximately

$$n_e(m\Delta t) \;=\; 213\,\left(1 - e^{-0.54\Delta t}\right)\left(e^{-0.54\Delta t}\right)^m \;, \qquad (27)$$

which has the same form as (26). Comparing the two equations, it is seen that for $N_r = 213$ and $\Delta t = 1$ day, $1-P = \exp(-0.54)$, or $P = 0.42\ \mathrm{d}^{-1}$. It may be verified from (1) and (27) that in the limit $t = m\Delta t \to \infty$, the average time for a weakened locality to fail is 2.4 days; that is, the probability of failure in 1 day is $P = 0.42$. The magnitude of $N_r = 213$ at Long Valley suggests that many bubbly regions are distributed throughout the geothermal field. A large fraction of these regions is presumed to be located in the approximately 200-km^3 region in the southeastern portion of the caldera centered at about 7 km depth where most of the triggered seismicity after the Landers earthquake occurred [*Hill et al.*, 1995], implying that in this location they are distributed on average with a 1-km spacing.

It is possible, or even likely, that triggered seismic events are not statistically independant as assumed in the above calculation; that is, triggered seismicity triggers seismicity [*Rice and Gu*, 1983]. Furthermore, relaxation by seismicity is coupled to the percolation mechanism. We have shown that the timescales for relaxation by permeability and by seismicity are approximately the same; they are also about the same as the timescale for the postearthquake deformation. Therefore it is likely that the above analysis applies to some composite of coupled relaxation processes.

Discussion

The assumptions made in this work in order of decreasing strength are (1) preexisting bubbles occur in localized sparsely distributed regions, (2) CO_2 is slightly supersaturated in water, (3) large mode conversion occurs in the geothermal field, (4) the shear velocity is low: 50 m/s in bubbly regions, (5) processes occur with widely disparate timescales, (6) the nonsteady diffusion layer in rectified diffusion is thin, (7) the geothermal fluid is a binary H_2O-CO_2 mixture, (8) the number of bubbles is constant, (9) liquid and rock are incompressible, (10) the vapor in bubbles is a perfect gas, (11) Henry's law, (12) Darcy's law, (13) D is computed from η using a modified Einstein relation, (14) the temperature is constant, (15) the steady diffusion layer in resorption is thick, and (16) the thermodynamic variables change by only small amounts.

It may be noted that the predominant 10-s period of the Landers S waves at MLAC actually exceeds the upper limit for the validity of the high-frequency, thin nonsteady diffusive layer assumption of *Hsieh and Plesset* [1961]. No simple analytical results are available which account for thick nonsteady diffusion layers, but clearly, the results derived using (4) will substantially overestimate the pore pressure increase when the fluid between bubbles becomes substantially depleted of CO_2, that is, when the distance between bubbles ℓ is smaller than the thickness of the nonsteady layer, $\ell < \sqrt{D/\omega}$, where ω is the seismic frequency. Accordingly, for 10-s period ($\omega = 0.63$/s), at 5.6 km depth and 250°C, the bubble spacing must be on average larger than 0.15 mm; that is, the bubble number density must be less than $n_b < 2.7 \times 10^{11}\ \mathrm{m}^{-3}$. Therefore, with $a = 13$ m, in each bubbly region the number of bubbles must be less than $N < 2.5 \times 10^{15}$.

The higher-order theory of *Fyrillas and Szeri* [1994], which accounts approximately for the development of a steady depletion layer outside the oscillating bubble, yields essentially the same result as simpler theories neglecting such a layer (compare Figure 5 of *Fyrillas and Szeri* [1994], with Figure 4 of *Eller* [1969]). Again, this imposes a restriction on the bubble spacing; in order that the fluid not be severely depleted of CO_2, $\ell > \sqrt{D\Delta t} = 1.1$ mm at 5.6 km depth and 250°C. This condition is more stringent than the one derived in the preceding paragraph, requiring that $n_b < 7.6 \times 10^8\ \mathrm{m}^{-3}$ and $N < 7.0 \times 10^{12}$. Neither of these constraints on bubble number density seems to be very strong.

Large-amplitude (nonlinear) oscillations of bubbles enhance rectified diffusion [*Eller and Flynn*, 1965; *Crum*, 1984], but dynamic strain in seismic waves remote from the source is so small (of order 10^{-5} in hydrothermal systems at Long Valley during the Landers earthquake) that nonlinear effects there are negligible.

Laboratory experiments [*Crum*, 1980] show that for large bubbles, observed bubble growth rate by rectified diffusion is up to 20 times greater than predicted by even the theory accounting for nonlinear effects [*Eller*, 1969]. *Fyrillas and Szeri* [1995] show that the discrepancy can be resolved by accounting for the effects of surfactants. Presumably, the concentration of surfactants at seismogenic depths is small, so we have neglected this effect.

We conclude that though the rate of pressure rise in earthquakes may be slightly overestimated because of the violation of the small diffusion layer assumption, so long as the above constraints on bubble separation are met, the simple Hsieh-Plesset theory [*Hsieh and Plesset*, 1961] is sufficient to give an order-of-magnitude estimate of the effects of rectified diffusion.

Very small amounts of vapor are pumped into bubbles

by the small strains of earthquakes (in our calculations the vapor density in bubbles increases by only 0.007% in 80 s at 5.6 km and 250°C), so the resorption time (equation (21)) is extraordinarily large. Because the pore pressure increase by rectified diffusion is larger for longer-duration shaking, sustained shaking, for example, by harmonic tremor at volcanos, might build very large pressure.

The mechanism by which rectified diffusion generates rapid increase of pore pressure during seismic shaking depends on the confluence of several favorable conditions, including the existence of thermodynamic conditions promoting supersaturation and the generation of small bubbles, bubble-containing zones distributed throughout the seismogenic zone, a velocity structure promoting large dynamic strain at depth, and, perhaps, a preexisting stress state relatively close to the threshold for the nucleation of earthquakes [*Anderson et al.*, 1994]. Though this might be taken to imply that the effect would be rather uncommon, such conditions seem to occur frequently in the western United States. Thus the consequences of pressure increase by rectified diffusion during seismic shaking are likely to be many and varied.

For example, *Gomberg and Davis* [1996] show that there is a threshold rate for seismicity at The Geysers, California, triggered not only by remote earthquakes but also by local energy production and earthquakes within the field. Frequency dependence implies a competition between a fast facilitating process and a slow inhibiting process. The rectified diffusion/percolation model embodies two such processes. This model also suggests that the brief response at The Geysers to the Landers earthquake in comparison to that at Long Valley (3 hours relaxation time versus 58 hours) may have been due to the fact that the rock there is more permeable or that, on average, the accumulations of bubbles are somewhat smaller. One is tempted to speculate whether these differences might be related to extensive energy production at The Geysers.

As a second example, *Johnson and McEvilly* [1995] describe transient earthquake sequences at Parkfield, California confined to small cells of 20–30 m diameter which diffusively spread on the time scale of minutes to days along the San Andreas Fault. These sequences occur in a zone of large V_p/V_s ratio and high attenuation, indicative of fluid-saturated rock. Evidence for geothermal activity in the area is expressed at the surface by warm or sulphurous springs at sites approximately 4 km (Smith Mountain), 11 km (Coalinga Mineral Spring) and 13 km (Table Mountain), from the fault, southeast and northwest of Parkfield. The model presented in this paper applies directly to those observations, and together they suggest that self-induced buildup of pore pressure can provide a positive feedback mechanism for generating seismicity. Sequences nucleating in 20-m-diameter cells at 10 km depth which last for a day [*Johnson and McEvilly*, 1995] are consistent with rectified diffusion in soil of permeability approximately 10^{-15} m^2 (1 mdarcy; equation (20)). These two examples suggest that interpretation of seismic observations by the rectified diffusion model may ultimately be useful for measuring rock permeability at depth. Tomographic studies of structure at The Geysers and Long Valley caldera, similar to those carried out at Parkfield, would be useful in interpreting triggered seismicity and validating the rectified diffusion model.

Rectified diffusion provides a natural explanation for why only the Landers earthquake caused triggered seismicity in Long Valley even though the dynamic strain caused by the Landers earthquake is only a factor of 2 larger than that caused by other earthquakes [*Johnston et al.*, 1995]. Since the magnitude of the Landers earthquake is larger than other events, the duration was also likely to be larger. In addition, since the total effect of rectified diffusion is proportional to the product $\delta^2\,\Delta t$, it should be expected that triggering will be very sensitive to seismic magnitude.

Conclusions

Triggered seismicity at Long Valley caldera began only 40 s after arrival of the S wave train from Landers [*Michael*, 1992]. The seismicity rate was initially maximum ($\sim$ 90 earthquakes of magnitude $M > 1$ during the first day) and then decreased exponentially with a time constant of 1.9 days [*Hill et al.*, 1995]. We have shown that rectified diffusion into small compressible inclusions (bubbles) is sufficient to induce seismically significant increase of pore pressure during the 80-s duration of the Landers earthquake. The resulting temporal pattern of the seismicity is consistent with the initial pressurization. For the values used in the present calculations the pore pressure at 5.6 km depth and 250°C is pumped up by 10-μm-diameter bubbles at the rate of 151 Pa/s to an increase of 12 kPa during 80 s of shaking. The time during which the elevated pressure persists after shaking stops is of order 50 hours. Times of this magnitude result for bubble clouds of the order of 26 m diameter. Since the holding time τ (equation (20)) goes like a^2/κ, bubbly regions larger than 26 m diameter will hold the pressure for as long in rock considerably more permeable. The parameters $\dot{p}_0$, the rate of pressure buildup, and t_r, the time to redissolve the volatile back into the liquid, are strongly dependent on the bubble radius r_0, smaller bubbles being favored for rapid pressure buildup. Observations of earthquake swarms at other locations suggest that self-induced buildup of pore pressure by rectified diffusion can provide a positive feedback mechanism for amplifying seismicity.

Appendix: Distribution of Bubble Sizes

In this section we describe the effects of a distribution of $N_i(r_i)$ bubbles each of radius r_i (volume, $V_{ib} = (4\pi/3)r_i^3$) in a bubbly region of radius a. The

distribution of bubble sizes is taken to be discrete, with k different size classes, such that

$$N = \sum_{i=1}^{k} N_i \tag{A1}$$

$$V = \sum_{i=1}^{k} N_i V_{ib} = \frac{4}{3}\pi N \overline{r^3}\,, \tag{A2}$$

where the bar denotes the mean value, as in

$$\overline{r} = \frac{1}{N}\sum_i N_i r_i\,. \tag{A3}$$

For $N_i = \text{const}$, equation (A2) gives

$$\dot{V} = \sum_i N_i \dot{V}_{ib}\,. \tag{A4}$$

equation (10) written for V_{ib}, with equation (8), is

$$\frac{\dot{p}}{p_0} = -\frac{\dot{V}_{ib}}{V_{ib0}} + \frac{K}{r_{i0}^2}\,. \tag{A5}$$

If $\dot{V}$ is taken to be known (see equation (12)), (A4) and (A5) are $k+1$ equations for the $k+1$ unknowns $(\dot{V}_{ib}, \dot{p})$. The pressure generated by the entire population of bubbles can be calculated by solving (A5) for $\dot{V}_{ib}$, multiplying by N_i, summing, and applying (A2)–(A4), with the result

$$\frac{\dot{p}}{p_0} = -\frac{\dot{V}}{V_0} + K\frac{\overline{r_0}}{\overline{r_0^3}}\,. \tag{A6}$$

Thus, by comparing (A6) with (11), it can be seen that the effective radius r_{eff}, namely, the radius of a monodisperse distribution of preearthquake bubbles which generates the same rate of pressure increase as the distribution $N_i(r_i)$, is

$$r_{\text{eff}} = \left(\frac{\overline{r_0^3}}{\overline{r_0}}\right)^{\frac{1}{2}}\,. \tag{A7}$$

The effective radius is weighted by the third moment in the numerator, toward larger, slower growing bubbles. Thus $\dot{p}$ for a distribution of bubble sizes is smaller than that given by (11) if the mean radius of the distribution is used.

The time for resorption (equation (23)) can be rederived from (21) accounting for a distribution of bubble sizes by using the same procedure as for (A6). The result is

$$\overline{t_r} = \frac{\overline{r_0^4}}{\Delta t}\left(\frac{\rho_{0v}}{6\,D\,C_\infty\,\delta}\right)^2 = \frac{\overline{r_0^4}}{r_0^4}\frac{p_0^2}{\dot{p}_0^2}\frac{1}{\Delta t}\,. \tag{A8}$$

Comparing with (23), it can be seen that the resorption time is even more strongly biased toward the larger, slower bubbles than is $\dot{p}$.

During the earthquake, rectified diffusion tends to equalize the size of the bubbles in a process analogous, but inverse, to Ostwald ripening [*Cheng and Lemlich*, 1985]. Small bubbles grow at the expense of large bubbles. To illustrate the effects of the ripening process we consider a simplified constant-volume system (no liquid leakage or compressibility, $\dot{V} = 0$). From (A5) and (A6) with $\dot{V} = 0$ the time t_{ij} at which the class of bubbles with initial radius r_{i0} reaches the size of bubbles initially with radius r_{j0} is

$$t_{ij} = \left[K\left(\frac{r_{i0} - r_{j0}}{r_{i0}^3 - r_{j0}^3} + \frac{1}{r_{\text{eff}}^2}\right)\right]^{-1}\,, \tag{A9}$$

and their common radius at that time is

$$\frac{r_i(t_{ij})}{r_{i0}} = \left(1 + \frac{\dfrac{1}{r_{i0}^2} - \dfrac{1}{r_{\text{eff}}^2}}{\dfrac{r_{i0} - r_{j0}}{r_{i0}^3 - r_{j0}^3} + \dfrac{1}{r_{\text{eff}}^2}}\right)^{\frac{1}{3}}\,. \tag{A10}$$

Appendix B: Compressibility Effects

In this section show how the effects of liquid-phase compressibility may be accounted for. By conservation of volume the increase of the volume of vapor is equal to the compression of the liquid by the increased pore pressure plus the volume vacated by liquid percolation. That is, (12) becomes

$$\frac{\dot{V}}{V} = \beta\phi\dot{p} + \nabla\cdot u_r\,, \tag{B1}$$

where β is the liquid compressibility and ϕ is the porosity of the fractured rock matrix. Completing the derivation as in the body of the paper, (14) becomes

$$\frac{\partial p}{\partial t} - \frac{p_0\kappa/\eta}{1+p_0\beta\phi}\frac{1}{r^2}\frac{\partial}{\partial r}\left(r^2\frac{\partial p}{\partial r}\right) = \frac{\dot{p_0}}{1+p_0\beta\phi}\,, \tag{B2}$$

The equation is changed by the appearance of the factor $(1+p_0\beta\phi)$, which measures the magnitude of liquid compressibility relative to the vapor compressibility $(1/p_0)$, in the second and third terms.

At $p = 150$ MPa and $T = 250°$, for $\beta = 0.4\times10^{-9}$ Pa^{-1} and $\phi = 0.1$, $p_0\beta\phi \sim 0.007$, so the compressibility of water is negligible. In the solution (equation (16)) the definition of the parameter $p_{\max}$ is unchanged, while the similarity variable y becomes

$$y = \frac{a}{2}\sqrt{\frac{1+p_0\beta\phi}{p_0(\kappa/\eta)\,t}}\,. \tag{B3}$$

The small-time limit of the solution of (B2) becomes

$$p(0,t) - p_0 = \frac{\dot{p_0}\,t}{1+p_0\beta\phi}\,, \tag{B4}$$

while at large times the pressure approaches the same constant value $p_{\max}$, unaffected by liquid compressibility. The percolation time becomes

$$\tau = \frac{a^2(1+p_0\beta\phi)}{4p_0\kappa/\eta}. \quad \text{(B5)}$$

When the liquid compressibility is small ($p_0\beta\phi \ll 1$), we recover the results given in the body of the paper, and when the liquid compressibility times the porosity is large ($p_0\beta\phi \gg 1$), the group $1/\beta\phi$ replaces p_0 in the results.

Acknowledgments. The authors thank Egill Hauksson for providing accelerograms of the Landers earthquake recorded in Long Valley and D. P. Hill for a useful review of an early version of this paper. Reviews by A. T. Linde and an anonymous reviewer helped clarify many important points. This paper is based upon work supported under a National Science Foundation Graduate Fellowship and it is contribution 5662 of the Division of Geological and Planetary Sciences, California Institute of Technology.

References

Addo, K. O., and P. K. Robertson, Shear-wave velocity measurement of soils using Rayleigh waves, *Can. Geotech. J. 29*, 558-568, 1992.

Anderson, J. G., J. N. Brune, J. Louie, Y. Zeng, M. Savage, G. Yu, Q. Chen, and D. dePolo, Seismicity in the western Great Basin apparently triggered by the Landers, California, earthquake, June 28, 1992, *Bull. Seismol. Soc. Am., 84*, 863-891, 1994.

Blanchard, F. G., and P. Byerly, A study of a well gage as a seismograph, *Bull. Seismol. Soc. Am., 25*, 313-321, 1935.

Bodin, P., and J. Gomberg, Triggered seismicity and deformation between the Landers, California and Little Skull Mountain, Nevada, earthquakes, *Bull. Seismol. Soc. Am., 84*, 835-843, 1994.

Bowers, T.S., and H. C. Helgeson, Calculations of the thermodynamic and geochemical consequences of nonideal mixing in the system H_2O-CO_2-NaCl on phase relations in geologic systems: equation of state for H_2O-CO_2-NaCl fluids at high pressures and temperatures, *Geochim. Cosmochim. Acta, 47*, 1247-1275, 1983.

Carlslaw, H. S., and J. C. Jaeger, *Conduction of Heat in Solids*, 2nd ed., Oxford Univ. Press, New York, 1959.

Carragan, W., F. Michalko, and S. Katz, Water wells in earthquake and explosion detection, *Rep. AFCRL-64-177*, Off. of Aerosp. Res., U.S. Air Force, Bedford, Mass., 1964.

Cheng, H. C., and R. Lemlich, Theory and experiment for interbubble gas diffusion in foam, *Ind. Eng. Chem. Fundam., 24*, 44-49, 1985.

Crum, L. A., Measurements of the growth of air bubbles by rectified diffusion, *J. Acoust. Soc. Am., 68*, 203-211, 1980.

Crum, L. A., Rectified diffusion, *Ultrasonics, 22*, 215-223, 1984.

Delaney, P. T., Rapid intrusion of magma into wet rock: Groundwater flow due to pore pressure increases, *J. Geophys. Res., 87*, 7739-7756, 1982.

Eller, A., Growth of bubbles bectified diffusion, *J. Acoust. Soc. Am., 46*, 1246-1250, 1969.

Eller, A., and H. G. Flynn, Rectified diffusion during nonlinear pulsations of cavitation bubbles, *J. Acous. Soc. Am., 37*, 493-503, 1965.

Epstein, P. S., and M. S. Plesset, On the stability of gas bubbles in liquid-gas systems, *J. Chem. Phy., 18*, 1505-1509, 1950.

Flowers, G.C., Correction of Holloway's (1977) adaptation of the modified Redlich-Kwong equation of state for calculation of the fugacities of molecular species in supercritical fluids of geologic interest, *Contrib. Mineral. Petrol., 69*, 315-318, 1979.

Fyrillas, M. M., and A. J. Szeri, Dissolution or growth of soluble oscillating bubbles, *J. Fluid Mech., 277*, 381-407, 1994.

Fyrillas, M. M., and A. J. Szeri, Dissolution or growth of soluble oscillating bubbles: The effect of surfactants, *J. Fluid Mech., 289*, 295-314, 1995.

Gomberg, J., and S. Davis, Stress/strain changes and triggered seismicity at The Geysers, California, *J. Geophys. Res., 101*, 733-749, 1996.

Haar, L., J. S. Gallagher, and G. S. Kell, *NBS/NRC Steam Tables*, Hemisphere, New York, 1984.

Heaton, T. H., Tidal triggering of earthquakes, *Bull. Seismol. Soc. Am., 72*, 2181-2200, 1982.

Hill, D. P., et al., Seismicity remotely triggerd by the magnitude 7.3 Landers, California, earthquake, *Science, 260*, 1617-1623, 1993.

Hill, D. P., M. J. S. Johnston, and J. O. Langbein, Response of Long Valley caldera to the $M_w = 7.3$ Landers, California, earthquake, *J. Geophys. Res., 100*, 12,985-13,005, 1995.

Himmelblau, D. M., Diffusion of dissolved gases in liquid, *Chem. Rev., 64*, 527, 1964.

Hsieh, D.-Y., and M. S. Plesset, Theory of rectified diffusion of mass into gas bubbles, *J. Acoust. Soc. Am., 33*, 206-215, 1961.

Johnson, P.A., and T. V. McEvilly, Parkfield seismicity: Fluid-driven?, *J. Geophys. Res., 100*, 12,937-12,950, 1995.

Johnston, M. J. S., D. P. Hill, A. T. Linde, J. Langbein, and R. Bilham, Transient deformation during triggered seimicity from the June 28, 1992, $M_w = 7.3$ Landers earthquake at Long Valley volcanic caldera, California, *Bull. Seismol. Soc. Am., 85*, 787-795, 1995.

Kieffer, S. W., Sound speed in liquid-gas mixtures: Water-air and water-steam, *J. Geophys. Res., 82*, 2895-2904, 1977.

Klein, F. W., Earthquake swarms and the semidiurnal solid earth tide, *Geophys. J. R. Astron. Soc., 45*, 245-295, 1976.

Linde, A.T., I. S. Sacks, M. J. S. Johnston, D. Hill, and R. G. Bilham, Increased pressure from rising bubbles as a mechanism for remotely triggered seismicity, *Nature, 371*, 408-410, 1994.

Liu, H-L., Interpretation of near-source ground motion and implications, Ph.D. thesis, Calif. Inst. of Technol., Pasadena, 1983.

Matuzawa, T., *Study of Earthquakes*, 213 pp., Uno Shoten, Tokyo, 1964.

Mauk, F. J., and J. Kienle, Microearthquakes at St. Augustine Volcano, Alaska, triggered by Earth tides, *Science, 182*, 386-389, 1973.

Michael, A., Initiation of seismicity remotely triggered by the Landers earthquake: Where and when? (abstract), *Eos Trans. AGU, 73(43)*, Fall Meet. Suppl., 392-393, 1992.

Newhall, C. G., and E. Dzurisin, Historical unrest at large calderas of the world, *U.S. Geol. Surv. Prof. Paper 1855*, 1988.

Puzyrev, N. N., and V. A. Kulikov, Experimental data on the propagation and excitation of transverse waves in water-saturated deposits, *Sov. Geol. and Geophys.*, Engl. Transl., *21*, 71-77, 1980.

Rexin, E. E., J. Oliver and D. Prentiss, Seismically-induced fluctuations of the water level in the Nunn-Bush well in Milwaukee, *Bull. Seismol. Soc. Am., 52*, 17-25, 1962.

Rice, J. R., and M. P. Cleary, Some basic stress diffusion solutions for fluid-saturated elastic porous media with compressible constituents, *Rev. Geophys., 14*, 227-241, 1976.

Rice, J. R., and J.-C. Gu, Earthquake aftereffects and trig-

gered seismic phenomena, *Pure Appl. Geophys.*, *121*, 187-219, 1983.

Roeloffs, E. A., W. R. Danskin, C. D. Farrar, D. L. Galloway, S. L. Hamlin, E. G. Quilty, H. M. Quinn, D. H. Schaefer, M. L. Sorey, and D. E. Woodcock, Hydrologic effects associated with the June 28, 1992 Landers, California earthquake sequence, *U.S. Geol. Surv. Open File Rep. 95-42*, 1995.

Romero, A. E., and V. McEvilly, Velocity structure of the Long Valley caldera from the inversion of local earthquake *P* and *S* travel times, *J. Geophys. Res.*, *98*, 19,869-19,879, 1993.

Rydelek, P. A., P. M. Davis, and R. Y. Koyanagi, Tidal triggering of earthquake swarms at Kilauea Volcano, Hawaii, *J. Geophys. Res.*, *93*, 4401-4411, 1988.

Sauck, W. A., The Brawley, California, earthquake sequence of January 1975 and triggering by Earth tides, *Geophys. Res. Lett.*, *2*, 506-509, 1975.

Scott, D. R., and D. J. Stevenson, Magma ascent by by porous flow, *J. Geophys. Res.*, *91*, 9283-9296, 1986.

Singh, S. K., E. Mena, and R. Castro, Some aspects of source characteristics of the 19 September 1985 Michoacan earthquake and ground motion amplification in and near Mexico City from strong motion data, *Bull. Seismol. Soc. Am.*, *78*, 451-477, 1988.

Sorey, M. L., and C. D. Farrar, A conceptual model of the hydrothermal system in Long Valley caldera, California, USA, in *Water-Rock Interaction*, edited by Y. K. Kharaka and A. S. Maest, pp. 1357–1362, A.A. Balkema, Rotterdam, Netherlands, 1992.

Sorey, M. L., R. E. Lewis and F. H. Olmstead, The hydrostatic system of the Long Valley caldera, California, USGS Prof. Paper 1044-A, 1978

Fluid mechanism of pressure rise in volcanic (magmatic) systems with mass exchange, Steinberg, G., A. Steinberg, and A. Merzhanov, *Mod. Geol.*, *13*, 274-285, 1989.

Sterling, A., and E. Smets, Study of Earth tides, earthquakes and terrestrial spectroscopy by analysis of the level fluctuations in a borehole at Heibaart (Belgium), *Geophys. J. R. Astron. Soc.*, *23*, 225-242, 1971.

Takenouchi, S., and G. C. Kennedy, The binary system H_2O-CO_2 at high temperatures and pressures, *Am. J. Sci.*, *262*, 1055-1074, 1964.

Wiebe, R., and V. L. Gaddy, The solubility of carbon dioxide in water at various temperatures from 12° to 40° and at pressures to 500 atmospheres: Critical phenomena, *J. Am. Chem. Soc.*, *62*, 815-817, 1940.

E. E. Brodsky and H. Kanamori, Seismological Laboratory, California Institute of Technology, Pasadena, California 91125 (e-mail: brodsky@seismo.gps.caltech.edu; hiroo@seismo.gps.caltech.edu)

B. Sturtevant, Graduate Aeronautical Laboratories, California Institute of Technology, Pasadena, California 91125 (e-mail: brad@galcit.caltech.edu)

(Received March 5, 1996; revised August 26, 1996; accepted August 29, 1996.)